Colloids and Surfaces B: Biointerfaces 189 (2020) 110841

Contents lists available at ScienceDirect

Colloids and Surfaces B: Biointerfaces

journal homepage: www.elsevier.com/locate/colsurfb

Influence of graphene oxide nanoparticles on the transport and cotransport of biocolloids in saturated porous media

Maria P. Georgopoulou[a], Vasiliki I. Syngouna[a,b], Constantinos V. Chrysikopoulos[a,*]

[a] School of Environmental Engineering, Technical University of Crete, 73100, Chania, Greece
[b] Department of Environment, Ionian University, 29100, Zakynthos, Greece

ARTICLE INFO

Keywords:
Escherichia coli
Enterococcus faecalis
Staphylococcus aureus
Graphene oxide
Quartz sand
Cotransport in porous media

ABSTRACT

This study examines the effect of graphene oxide (GO) nanoparticles (NPs) on the transport (individual species) and cotransport (simultaneous transport) of three biocolloids (*Escherichia (E.) coli, Enterococcus (E.) faecalis* and *Staphylococcus (S.) aureus*) in water saturated porous media. Flowthrough experiments were performed in 30-cm long laboratory columns packed with quartz sand. All of the experiments were conducted at room temperature (22 °C), pH = 7, and ionic strength I_s = 2 mM. The results from the cotransport experiments indicated that the mass recovery values for all biocolloids, calculated based on total biocolloid concentration in the effluent, were reduced in the presence of GO NPs. The strains *E. coli* and *E. faecalis* were shown to be more vulnerable to GO NPs than *S. aureus*. Temporal moments of the breakthrough concentrations suggested that the presence of GO NPs significantly influenced the fate and transport of the three biocolloids. Extended DLVO theory was used to quantify the various interaction energy profiles, based on electrokinetic and hydrodynamic measurements.

1. Introduction

Groundwater contamination by pathogenic biocolloids of human origin remains a challenging public health problem. Accidental or intentional introduction of microorganisms into groundwater occurs mainly due to improper sludge disposal (e.g., application of low-quality sewage sludge as soil improver), wastewater discharge, artificial groundwater recharge, uncontrolled sanitary landfill drainage, leakage of sewage networks and septic tanks, as well as agricultural and livestock activities [1–5].

The rapid development of nanotechnology has led to the inevitable introduction of engineered nanomaterials (ENMs) and nanoparticles (e.g. fullerenes, graphene oxides, carbon nanotubes) into the environment [6–8]. Graphene oxide (GO), an important derivative of graphene, due to its surface oxygen-bearing functional groups (i.e., epoxy, carbonyl and carboxyl groups), which can easily be dispersed in water, can create stable suspensions [9–11]. In suspended form, GO can interact with soil biocolloids, deposit on their cell surfaces, and in turn can reduce or inhibit their mobility in porous media. At the present time, the in situ measurement of ENMs in the environment remains analytically infeasible [12–14]. Therefore, there is no current information regarding the GO concentration and thus mathematical models are applied to predict its exposure concentrations in the environment [15]. Based on recent studies, GO can be toxic to microorganisms [11]. However, the effects of GO against human pathogens still remain contradictory [16]. Some studies reveal that bacteria could benefit from the presence of GO in solution, enhancing their proliferation, while other studies demonstrate that GO could exhibit antibacterial activity, through mechanisms such as cutting, wrapping, trapping and oxidative stress [17–19].

Numerous physico-chemical and biological factors that influence the transport and retention of biocolloids [20–25] and GO NPs [26–31] in porous media, have been explored extensively in the literature. In addition, more recent studies reveal that the cotransport of suspended clay particles and/or engineered nanoparticles with human pathogens in porous media, provoke alterations in biocolloidal motility, stability, surface charge, hydrophobicity and retention capacity, which in turn affect their resistance, inactivation and deposition onto the solid matrix [25,32–36]. Although the impact of GO NPs on inactivation, transport and deposition behavior of different pathogens in porous media has been thoroughly explored [37–42] the influence of GO NPs on the simultaneous transport (cotransport) of several different biocolloids remains unclear. Certainly, in real environmental systems, GO NPs are highly likely to simultaneously interact with more than one type of pathogens. To our knowledge the effects of GO NPs on transport and deposition of co-existing biocolloids has not been examined before. This paper focuses mainly on the effect of suspended GO NPs on fate and transport of the model biocolloids: *E. coli*, *E. faecalis*, and *S. aureus*,

* Corresponding author.
E-mail address: cvc@enveng.tuc.gr (C.V. Chrysikopoulos).

https://doi.org/10.1016/j.colsurfb.2020.110841
Received 17 September 2019; Received in revised form 28 December 2019; Accepted 1 February 2020
Available online 03 February 2020
0927-7765/

individually as well as simultaneously. The selected biocolloids are used as indicators of fecal pollution, because they are frequently associated with the occurrence of serious waterborne diseases [43].

2. Materials and methods

2.1. Preparation of bacterial suspensions

The Gram-negative *E. coli* strain (DMS 498) and the Gram-positive bacterial strains *E. faecalis* ATCC 14,506 and *S. aureus* (isolated from a poultry sample and biochemically identified based on the API® Staph Test Biomerieux protocol) were used as model bacteria in the experiments conducted in this study. Prior to each experiment, duplicates of bacterial cultures were prepared in sterile plates (petri dishes) containing non-selective growth medium (Nutrient Agar, code LAB008) and were incubated in an oven at 37 °C for 48 h. Well-isolated colonies of the above cultures were transferred to 20 mL of sterile phosphate-buffer solution (PBS) of low ionic strength (I_s = 2 mM) and neutral pH (pH = 7). The selected I_s value of the PBS solution was chosen in order to enhance the GO NPs suspension stability, by inhibiting its aggregation. It has been observed that GO NPs remain stable in solution at a lower I_s range (10^{-3} and 10^{-2} M KCl), while GO NPs become unstable and undergo aggregation when $I_s \geq 10^{-1.5}$ M KCl [26]. A similar trend was also observed by Chowdhury et al. [44]. Bacterial concentration in the suspensions was quantified based on the McFarland turbidity scale (McFarland Standard No. 0.5), according to which, 0.1 optical absorbance of a uniform microbial suspension at 600 nm corresponds to a concentration of ~ 10^8 CFU/mL [45,46]. A UV–vis spectrophotometer (UVmini-1240, Shimadzu) was used for the optical density measurements. A cell concentration of ~10^5 CFU/mL, which is commonly found in both raw and treated wastewater (depending on the type of treatment) [47], prepared by dilution of dense bacterial suspensions, was chosen as the initial bacterial concentration for both transport and cotransport column experiments.

2.2. Quantification of bacterial concentration

Bacterial concentrations of collected samples were determined by pouring a small amount (300 μL) of sample onto sterilized petri dishes containing a solid agar medium and counting the number of the formed bacterial colonies. The selective nutrient media Harlequin (*E. coli*/Coliform Medium, product code HAL008), Slanetz and Bartely Agar (code LAB166) and Mannitol Salt Agar were purchased in powder form for the growth of *E. coli*, *E. faecalis* and *S. aureus*, respectively. For each sample, duplicates of bacterial cultures were prepared by uniformly spreading 300 μL of the sample onto plates containing the appropriate solid growth substrate. Subsequently, the plates were incubated in an oven at 37 °C for 48 h (see Fig SI1). Depending on the sample concentration, multiple dilutions were performed with PBS. The number of colonies formed using 300 μL of sample was converted to number of colonies per 1 mL. Therefore, all bacteria concentrations were reported as colony-forming units per milliliter (CFU/mL) and represent the average of two replicate plates.

2.3. Preparation of GO NPs suspension

Prior to each experiment, a fresh suspension of dense GO NPs (100 mg/L) was prepared by ultrasonically dispersing a small mass (10 mg) of GO sheets (CAS No 763713, Sigma-Aldrich, St. Louis, USA) in appropriate volume of sterile PBS solution (100 mL). The duration of the sonication process (sonication bath Elmasonic S30/(H), Elma Schmidbauer GmbH, Singen, Germany, working at 37 kHz) was set to 2 h to ensure suspension uniformity [48,49]. The dense GO suspension was diluted with PBS solution, to achieve 20 mg/L initial GO NPs concentration, for both transport and cotransport experiments. The selected initial concentration of GO NPs (20 mg/L) is comparable to concentration values used in other published studies that simulate the filtration and mobility of GO NPs under various experimental conditions in columns packed with porous media (e.g., glass beads, silica sand, quartz sand, model soils) [50,51]. The optical density of GO NPs in the concentration range of 2 − 100 mg/L was analyzed at the optimal wavelength of 231 nm, using a UV–vis double-beam spectrophotometer (model UV-1900, Shimadzu). Then, a calibration curve (see Fig S2), correlating GO absorbance, Abs [-], with GO concentrations was created for pH = 7, and I_s = 2 mM.

Note that sterile ultrapure water (Easypure II, Barstead, U.S.A.) of specific resistivity of ~18.2 MΩ cm at 25 °C was used in the preparation of all working solutions and suspensions. Moreover, for the estimation the electrokinetic and hydrodynamic properties of GO NPs and each bacterium, under the specific experimental conditions (i.e., pH = 7, I_s = 2 mM, T = 22 °C), zeta potential (ζ), and hydrodynamic diameter (d_H) measurements of each working suspension were determined in triplicates with a zetasizer (Nano ZS90, Malvern Instruments, Southborough, MA). The zetasizer performs size measurements using a process called Dynamic Light Scattering (DLS). In particular, it measures Brownian motion, which is the movement of particles due to the random collision with the molecules of the liquid that surrounds the particle, and relates this to the size of the particles. The intensity-weighted distribution shows how well differently-sized particles are detected from a fit to the autocorrelation function of the measured scattering. In order to detect even small amounts of aggregation, an intensity distribution was chosen that could be highly sensitive to very small numbers of aggregates. The estimated numerical values are listed in Table S1.

2.4. Column characterization and experimental procedures

The experimental glass column (30-cm long, 2.5-cm diameter) and its accessories were sterilized by autoclave (120 °C) to minimize the possibility of microbial contamination. The initial net weight of column was determined (306.24 g ± 3.95 g). Then, using a vortex mixer, the column was filled and packed with coarse (0.850–1.000 mm, sieve No. 20) quartz sand (Filcom Filterzand and Grind, SiO_2 96.2 %), which was purified and sterilized according to the procedures described by Syngouna and Chrysikopoulos [32]. The bulk density of the packing material, the porosity, and the pore volume (PV) of the column were estimated to be: 1.75 ± 0.04 g/cm^3, 0.39 ± 0.02 [-], and 57.86 ± 2.04 mL, respectively. Note that the estimated porosity value coincides with values reported in the literature for quartz sand similar to the one used in this study [52]. The column was placed in the horizontal position to restrict possible gravity effects [53].

In order to mimic groundwater flow conditions, a slow volumetric discharge rate of 0.8 mL/min was chosen for all flowthrough experiments. This corresponds to an average seepage/interstitial velocity (i.e., Darcy velocity/porosity) of 0.44 cm/min. Four sets of transport experiments were conducted. Firstly, transport experiments were conducted to determine the individual transport characteristics of the three selected biocolloids. Subsequently, the transport of each pathogenic microorganism was investigated under simultaneous flow of a GO suspension, to identify any possible changes in motility and/or column retention of the biocolloids due to possible formation of biocolloid-GO NPs complexes. Additionally, cotransport experiments using simultaneously the three bacterial strains were performed in the presence and absence of a GO NPs suspension, in order to investigate any changes in bacterial cotransport and retention caused by the presence of GO NPs. Prior to each experiment, equilibration of the column was carried out by injecting 10 PVs of PBS using a peristaltic pump (Masterflex L/S, Cole-Palmer).

For the transport experiments, 3 PVs of each microbial suspension was pumped through the column. For the cotransport experiments, two separate input streams (i.e., microbial or combined microbial suspension and GO NPs suspension) were joined into a single input flux, and 3

PVs of the resulting combined suspension was injected into the column. For all experiments, after the injection of the 3 PVs of suspensions, 5 PVs of free PBS solution where injected to rinse the column. Column effluent samples (2 mL) were collected at pre-selected time intervals. Samples containing bacterial cells were stored at 4 °C to prevent possible cell proliferation prior to sample analysis.

2.5. Theoretical considerations

The nonlinear least squares regression software ColloidFit [54] was employed to fit the breakthrough data from the various biocolloid transport experiments. The mathematical model employed (eq SI1), originally proposed by Sim and Chrysikopoulos [55], describes the transport of suspended biocolloids in one-dimensional, water saturated, homogenous porous media, under uniform flow, accounting for first-order attachment kinetics and inactivation of biocolloids suspended in the aqueous phase and attached onto the solid matrix. The fitted parameters are presented in Table SI2. Note that the breakthrough data from the various biocolloid cotransport experiments were not fitted, because the fitting of complex cotransport breakthrough data still remains a nontrivial task. Also, the breakthrough data were subjected to first normalized temporal moment, M_1 [t], analysis, as described in eq SI12. In addition, quantification of the recovered mass, M_r, of the suspended biocolloids at the column exit was achieved with the software ColloidFit using the mathematical relationship (SI13) [56].

Quantification of microbial attachment onto quartz sand, both in absence and presence of GO NPs was achieved by applying the classical colloid filtration theory (CFT), assuming that the clean-bed filtration theory is valid (i.e. the subsequent deposition of bacteria is not influenced by already deposited bacteria) [24]. The dimensionless collision efficiency, α [-], which refers to the ratio of effective collisions to the total number of collisions occurring between suspended particles and collector grains was calculated from the breakthrough curves, based on the model proposed by Rajagopalan and Tien [57] and using the dimensionless single-collector removal efficiency, η_0, provided by Tufenkji and Elimelech [58] (see eqs SI14-SI28).

The extended Derjaguin-Landau-Verwey-Overbeek (XDLVO) theory was used to calculate the total interaction energy (Φ_{tot}) between bacteria and quartz sand, bacteria and bacteria, and GO and bacteria, as a function of separation distance h, by summing the van der Waals (Φ_{vdW}) attraction, the electrical double layer (Φ_{dl}) repulsion, Born (Φ_{Born}) repulsion, and the Lewis acid-base (Φ_{AB}) interaction energies [59], as outlined in the Supplementary data.

3. Results and discussion

3.1. Effect of GO NPs on biocolloid transport

Fig. 1 presents normalized breakthrough data for bacteria transport in the absence (open symbols) and presence (solid symbols) of GO NPs for (a) *E. coli*, (b) *E. faecalis*, and (c) *S. aureus*. The corresponding M_r values are listed in Table 1. In the absence of GO NPs, the estimated M_r values for *S. aureus* were lower than those of *E. faecalis* and *E. coli*. These findings are consistent with the ColloidFit results (see Table SI2), which confirm that the attachment rate constant ($r_{b\text{-}b^*}$) for *E. coli* to sand is the lowest among the three bacteria examined. In fact, the model parameters obtained through fitting of the transport data (see Table SI2) suggested that the *E. coli* detachment rate from quartz sand was the highest, while the inactivation rate for *E. coli* both in suspension and attached onto the solid phase were the lowest among the bacteria examined. In contrast, *E. faecalis* and *S. aureus* exhibited higher deposition rates and hence stronger irreversible attachment. In general, *E. coli* is known to exhibit relatively poor attachment onto solid surfaces [60]. Furthermore, *S. aureus* is less negatively charged than the other two bacteria examined at the experimental conditions of this study (see Table S1). The bacterial transport ability is correlated to cell surface

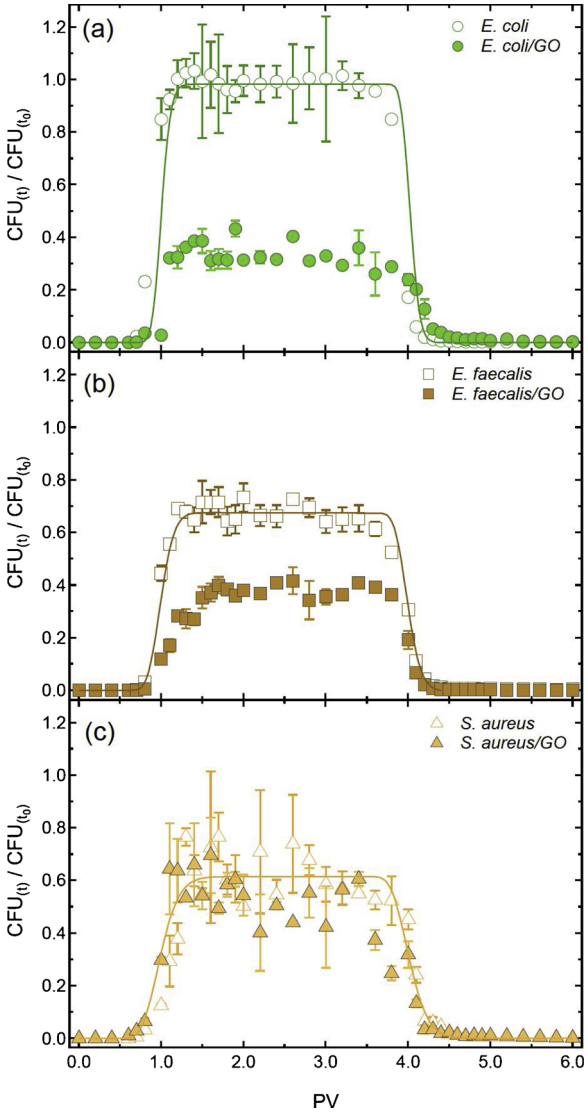

Fig. 1. Normalized experimental concentrations (symbols) with SD values (error bars) for N = 3, and fitted predictions (curves) of the transport of: (a) *E. coli*, (b) *E. faecalis*, and (c) *S. aureus*, in the absence of GO NPs (open symbols), and in the presence of GO NPs (solid symbols). Error bars not shown are smaller than the size of the symbol.

charge [61]. Thus, *S. aureus* was expected to attach onto quartz sand more than the other two bacterial strains. Consequently, the low M_r values observed for *S. aureus* may be attributed to its higher attachment and inactivation rates (see Table S2). Moreover, the transport of GO NPs through the column was greater in the absence of bacterial strains with an estimated M_r value of 83.1 % (see Fig SI3, Table 1). Conversely, the corresponding M_r values of GO NPs in the presence of *E. coli* and *E. faecalis* were 48.5 % and 68.8 %, respectively. Finally, in the presence of *S. aureus*, only 16.1 % of the injected GO NPs were recovered, suggesting that among the three bacteria, *E. faecalis* influences less the transport and retention of GO NPs. The presence of bacterial strains may increases the charge (less negative) of the quartz sand [62], resulting in greater quartz-GO NPs interactions and subsequent GO NP retention in the column. These results agree with prior nanoparticle studies which have shown that near neutral particles tend to be reversibly bound [63,64]. In addition, the shape irregularity and surface roughness of sand grains were expected to affect straining strength of each bacterium, which also depends on bacteria-bacteria and bacteria-sand interaction energies [65,66]. The calculated first normalized

Table 1
Experimental conditions and estimated parameter values.

Number of Experiment	Experimental conditions		θ [-]	q $\times 10^{-5}$ [m/s]	First normalize Moment M_1 (min)	Mass recovery [%]	RC [-] C_{bss} / C_{b0}	η_0 [-]	α [-]	η [-]
Transport										
1	*E. coli*		0.38	2.80	173.1	98.2	0.98	7.49×10^{-3}	7.32×10^{-3}	5.48×10^{-5}
2	*E. faecalis*		0.39	2.71	176.3	67.1	0.66	8.37×10^{-3}	1.59×10^{-1}	1.33×10^{-3}
3	*S. aureus*		0.38	2.70	175.4	61.5	0.71	1.48×10^{-2}	7.45×10^{-2}	1.10×10^{-3}
4	GO		0.38	2.72	185.5	83.1	0.85	1.58×10^{-2}	3.31×10^{-2}	5.24×10^{-4}
Cotransport										
5	*E. coli/E. faecalis /S. aureus*	*E. coli*	0.41	2.70	188.4	100.3	0.91	7.40×10^{-3}	4.20×10^{-2}	3.11×10^{-4}
		E. faecalis			190.3	64.8	0.67	8.12×10^{-3}	1.67×10^{-1}	1.35×10^{-3}
		S. aureus			182.2	68.3	0.86	1.42×10^{-2}	3.64×10^{-2}	5.18×10^{-4}
Cotransport in presence of GO										
6	*E. coli*/GO	*E. coli*	0.39	2.62	190.0	32.8	0.32	7.85×10^{-3}	4.67×10^{-1}	3.67×10^{-3}
		GO			185.8	48.5	0.47	1.63×10^{-2}	1.52×10^{-1}	2.47×10^{-3}
7	*E. faecalis*/GO	*E. faecalis*	0.40	2.76	187.5	36.1	0.37	8.04×10^{-3}	4.16×10^{-1}	3.34×10^{-3}
		GO			194.4	68.8	0.68	1.53×10^{-2}	8.59×10^{-2}	1.31×10^{-3}
8	*S. aureus*/GO	*S. aureus*	0.41	2.69	182.3	52.7	0.40	1.42×10^{-2}	2.16×10^{-1}	3.08×10^{-3}
		GO			178.8	16.1	0.25	1.55×10^{-2}	3.03×10^{-1}	4.69×10^{-3}
9	*E. coli/E. faecalis /S. aureus*/GO	*E. coli*	0.40	2.71	182.7	55.3	0.58	7.46×10^{-3}	2.43×10^{-1}	1.81×10^{-3}
		E. faecalis			192.3	44.5	0.48	8.17×10^{-3}	3.02×10^{-1}	2.47×10^{-3}
		S. aureus			180.4	46.1	0.60	1.43×10^{-2}	1.21×10^{-1}	1.73×10^{-3}
		GO			185.1	36.4	0.43	1.55×10^{-2}	1.79×10^{-1}	2.78×10^{-3}

temporal moments, which defines the mean breakthrough time or average velocity, were found to be higher for *E. faecalis* than S. *aureus and E. coli* (see Table 1). In addition, the *E. coli* strain used in this study possesses flagella; thus, the lower M_1 value determined for *E. coli* could be attributed to its cellular motility. Chemotaxis has been found to be an important mechanism influencing bacterial transport through soils, especially at low flow rates [67–69]. Note that, at the same I_s, motile bacteria have shown greater adhesion to the surface of collectors than nonmotile bacteria [70]. The M_r values, listed in Table 1, as calculated with eq (SI13), were considerably reduced in the presence than the absence of GO NPs. The calculated first normalized temporal moment, which defines the mean breakthrough time or average velocity, was found to be higher for *E. faecalis* than *S. aureus* and *E. coli* (see Table 1). The calculated M_r values in the presence of GO NPs was reduced more for *E. coli* (-66.6 %) than *E. faecalis* (-46.2 %) and *S. aureus* (-14.3 %), suggesting that *S. aureus* transport was affected relatively less by the presence of GO NPs. The GO NPs were expected to be both suspended in the liquid phase and attached onto the quartz sand. Consequently, GO NPs could heteroaggregate to form GO NPs-bacteria complexes, which can significantly affect bacteria transport and attachment. This assumption is consistent with the results reported by Peng et al. [71]. Note that the mean breakthrough time (M_1) was found to be higher for *E. coli* than *E. faecalis* and S. *aureus*. Also, the presence of GO NPs increased the mean breakthrough time of all three bacteria examined in this study (see Table 1).

3.2. Effect of GO NPs on biocolloid cotransport

Fig. 2 presents normalized breakthrough data for bacteria cotransport in the absence (Fig. 2a) and presence (Fig. 2b) of GO NPs. The corresponding M_r values are listed in Table 1. The estimated M_r values for *E. faecalis* in the absence of GO NPs were lower than those of *S. aureus* and *E. coli*. Moreover, the simultaneous transport of bacteria (cotransport) contributed to a reduction in M_r values for *E. faecalis* (-3.43 %) and to an enlargement in M_r values for *E. coli and S. aureus* (+2.14 % and +11.10 %, respectively). Chen and Walker [72] found that *E. faecalis* would preferentially attach at the air/water interface, whereas *E. coli* showed similar affinity to the air/water interface and to the sand surface, suggesting that different bacterial strains have different transport behavior in porous media. Note that, biocolloids attached onto the solid matrix could possibly act as additional collectors creating multi layered biofilms [73]. Thus, the presence of multiple

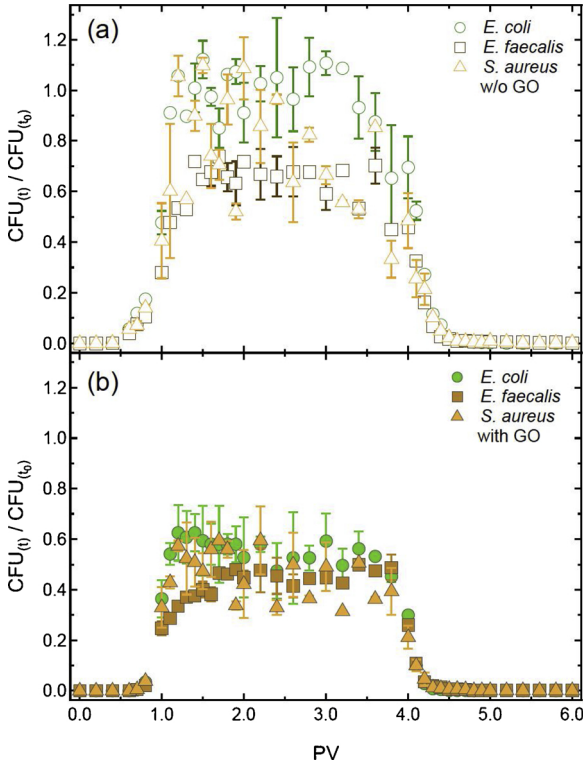

Fig. 2. Normalized experimental concentrations (symbols) with SD values (error bars) for N = 3, of the cotransport of *E. coli* (circles), *E. faecalis* (squares), and *S. aureus* (triangles): (a) in the absence of GO NPs, and (b) in the presence of GO NPs. Error bars not shown are smaller than the size of the symbol.

bacterial strains on the surface of the quartz sand may alter the properties or physicochemical characteristics of the solid matrix surfaces [74–76]. Also, the presence of multiple suspended bacterial strains may lead to competitive attachment and enhanced bacterial transport due to blocking [73].

The observed enhancement of *E. coli and S. aureus* migration during cotransport could be attributed to an increase in bacteria-sand repulsion caused by the enhanced negative surface charge of the sand due to previously deposited bacterial strains. Moreover, Whitman et al. [77] suggested that quorum sensing among bacteria could affect their release

from the sand. Furthermore, the mean breakthrough time of bacteria cotransport was found to be higher for *E. coli* than *E. faecalis* and S. *aureus* (see Table 1). Clearly, the presence of multiple bacterial strains hindered their migration and increased their mean breakthrough time (+15.27 min for *E. coli,* +14.05 min for *E. faecalis,* and +6.8 min for S. *aureus*).

In the presence of GO NPs all bacteria exhibited a considerable reduction in M_r, compared to the corresponding values obtained in the absence of GO NPs (see Table 1). Note that Gram-negative bacteria, i.e. *E. coli,* have been shown to be more resistant to inactivation, caused by GO NPs than Gram-positive bacteria such as *E. faecalis* and *S. aureus* [78]. However, the M_r reduction due to the presence of GO NPs was greater for *E. coli* (-44.90 %) than *E. faecalis* (-31.30 %) and *S. aureus* (-32.50 %). Worthy to note is that the presence of GO NPs affected more the bacterial transport than the bacterial cotransport, except for the case of *S. aureus*. Finally, the estimated M_r value (36.4 %) for GO NPs in the simultaneous presence of bacterial strains was found to be lower than that in the absence of them (83.1 %) (see Fig SI3, Table 1).

3.3. CFT results

The collision efficiency values, α, based on total bacterial concentration in the effluent, calculated with eq (SI14) for all three bacteria, are listed in Table 1. The α values for *E. faecalis* for both transport and cotransport experiments were higher than those of *S. aureus and E. coli* (see Table 1, Fig. 3a and b). Moreover, for both bacterial transport and cotransport experiments, α values were higher in the presence of GO NPs, which indicates that GO NPs significantly enhanced the bacterial collision efficiencies. For bacterial transport in the presence of GO NPs, the observed α values were slightly higher for *E. coli* indicating greater affinity of *E. coli* for GO particles than the other two bacteria; while for bacterial cotransport in the presence of GO NPs, the highest α values were observed for *E. faecalis*, probably due to the greater affinity of *E. faecalis* for GO particles [79]. If a collector becomes partly blocked by the presence of attached bacteria and GO NPs, α may either increase or decrease when additional bacteria and GO NPs are added, depending on whether GO-GO, bacteria-bacteria and GO-bacteria attachment is favourable or unfavourable [42,80]. Also, the collision efficiency between biocolloids and porous media may have been enhanced by the surface roughness of the quartz sand [81].

3.4. XDLVO results

The Φ_{tot} interaction energies between each of the three bacteria considered in this study and the quartz sand, assuming a sphere-plate approximation, normalized by the product of the Boltzmant constant (k_B) and the temperature (T), estimated as a function of separation distance, for the experimental conditions (PBS solution, pH = 7, I_S = 2 mM), are shown in Fig. 4a. Note that the electrokinetic ζ-potentials listed in Table SI1 were used instead of the surface potentials. Clearly, it is evident that the XDLVO interaction energies were highly repulsive for relatively long separation distances. The Φ_{tot} profiles of bacteria-sand interactions exhibited energy barriers ranging from Φ_{max1} = 77.14–425.60 k_BT, with the highest energy barrier observed for *E. faecalis*. Thus, it was almost impossible for the three bacterial strains to overcome the imposed Φ_{max1} and to attach onto the sand surfaces in the deep primary minima, Φ_{min1}. However, the surface roughness of the quartz sand grains has been found to reduce the energy barrier between cells and the solid surface [82–84]. Moreover, the XDLVO curves showed the presence of secondary minima, Φ_{min2}, indicating unfavourable attachment (attachment in the Φ_{min2}). All calculated Φ_{max1}, Φ_{min1}, and Φ_{min2} values were listed in Table SI3.

Hydrophobic interactions have been found to greatly affect bacterial adhesion [85–88]. Thus, for the evaluation of Lewis acid-base free energy of interaction $\Phi_{AB(h=h_0)}$ [J/m^2] between the three bacteria examined and the quartz sand at a separation distance h = 0.25 nm, the Yoon et al. [89] empirical approach (SI41) was employed with hydrophobic force constants predicted by the empirical relationship (SI42).

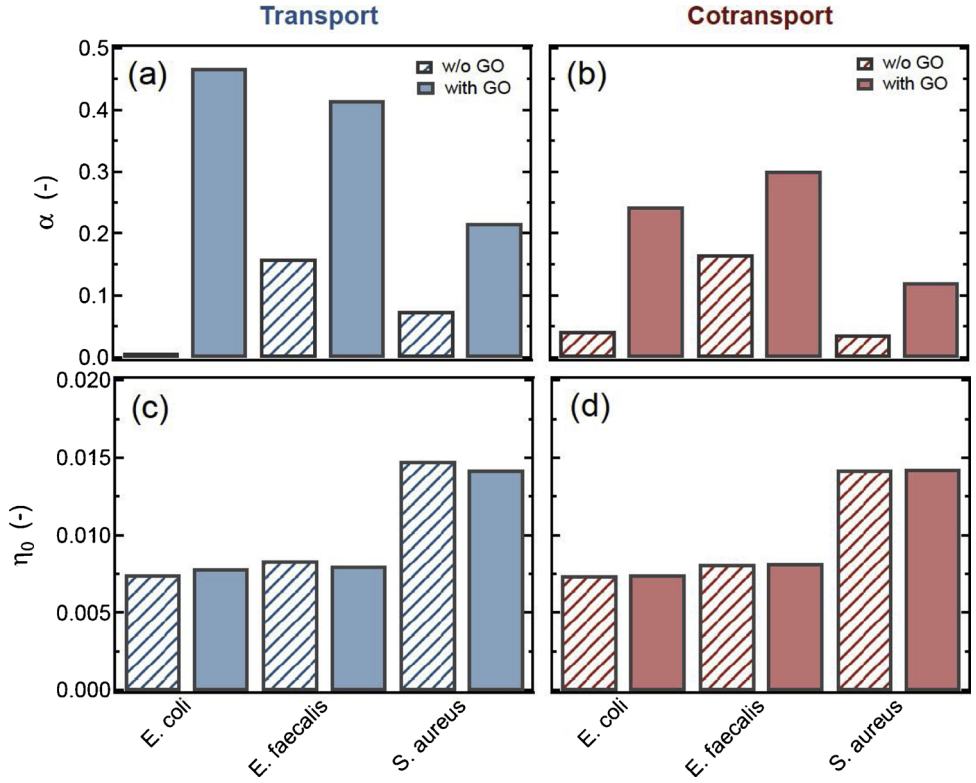

Fig. 3. Calculated values for: (a,b) collision efficiency, α, based on the total biocolloid concentration in the effluent, and (c,d) single-collector contact efficiency, η_0, for microbial: (a,c) transport, and (b,d) cotransport experiments, both in the absence and presence of GO NPs.

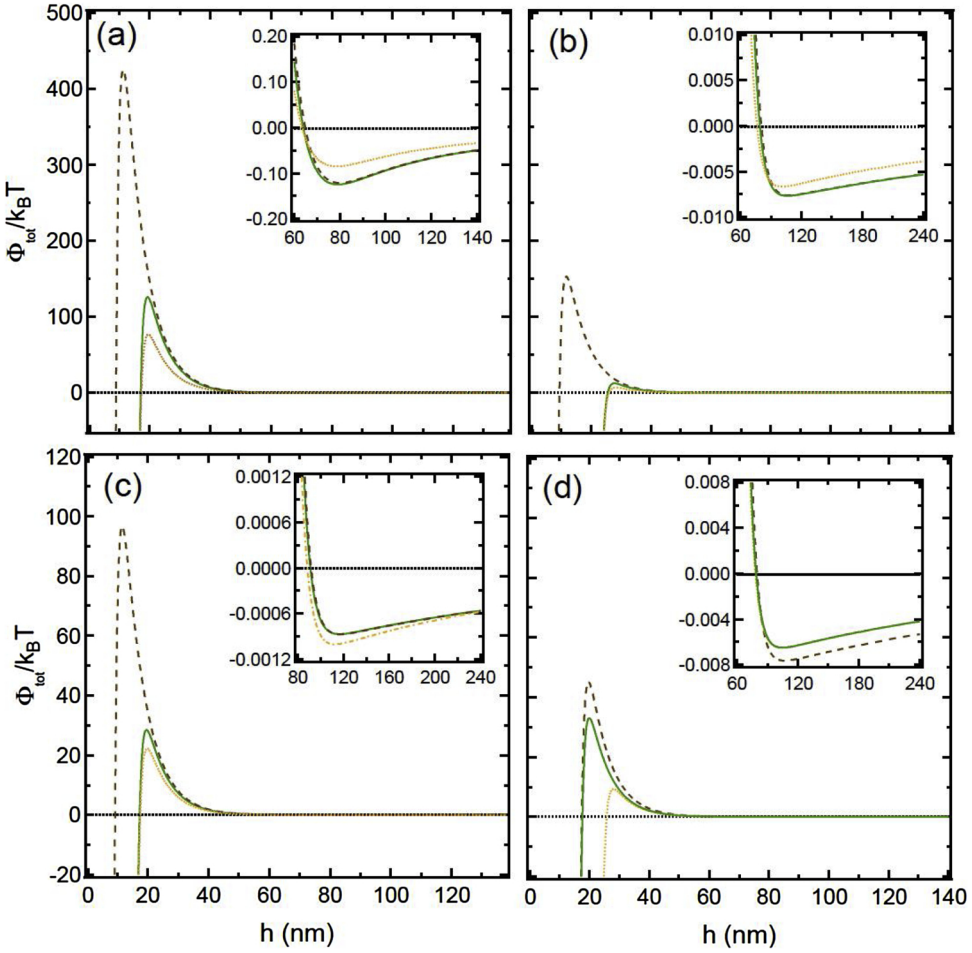

Fig. 4. Predicted XDLVO total energy profiles as function of separation distance for the pairs: (a) *E. coli*-sand (continuous curve), *E. faecalis*-sand (dashed curve) and *S. aureus*-sand (dashed – dotted curve); (b) *E. coli*-*E. coli* (continuous curve), *E. faecalis*-*E. faecalis* (dashed curve) and *S. aureus*-*S. aureus* (dotted curve); (c) *E. coli*-GO (continuous curve), *E. faecalis*-GO (dashed curve), and *S. aureus*-GO (dotted curve); (d) *E. coli*-*E. faecalis* (dashed curve), *E. coli*-*S. aureus* (dotted curve), *S. aureus*-*E. faecalis* (continuous curve). Each figure insert highlights the corresponding secondary energy minima (Φ_{min2}).

The various $\Phi_{AB(h=h_o)}$ values calculated are listed in Table SI3. It is worth to mention that $\Phi_{AB(h=h_o)}$ value was slightly more negative for *S. aureus* (-4.876×10^3 J/m^2) than *E. coli* (-4.231×10^3 J/m^2) interactions with the quartz sand (see Table SI3). The $\Phi_{AB(h=h_o)}$ value for *E. faecalis* interaction with the quartz sand was found to be -4.472 J/m^2. These findings are in agreement with the experimental results of this study (see Fig. 1 and Table 1), which suggested that *S. aureus* deposition onto quartz sand was higher than of *E. coli* and *E. faecalis*.

The Φ_{XDLVO} profiles for the case of sphere-sphere approximation (eqs SI34-SI39) as applied to homoaggregation (bacteria-bacteria) were shown in Fig. 4b, and heteroaggregation (GO-bacteria and bacteria-bacteria) were shown in Fig. 4c,d, respectively. Clearly, the profiles in Fig. 4b indicated that no coagulation occurred between *E. faecalis* particles (high energy barrier of Φ_{max1} = 153 k_BT) under the experimental conditions. These observations suggested that the *E. faecalis* suspension was stable under the experimental conditions. Note that *E. coli* and *S. aureus*, were expected to homoaggregate due to low energy barriers (Φ_{max1} = 12.71 k_BT, and Φ_{max1} = 7.09 k_BT, respectively). The highest Φ_{max1} (97.61 k_BT) was observed for GO-*E. faecalis* interactions, while the lowest Φ_{max1} (22.40 k_BT) was observed for GO-*S. aureus* interactions. The profiles in Fig. 4d show that the calculated energy barriers, Φ_{max1}, are higher for *E. coli*-*E. faecalis* (45.11 k_BT) and *E. faecalis*-*S. aureus* (33.08 k_BT) than *E. coli*-*S. aureus* (9.308 k_BT) (see Fig. 4c and Table SI2). Therefore, heteroaggregation is more possible to occur between *E. coli* and *S. aureus*.

4. Conclusions

It was observed that the transport and cotransport of bacterial strains (*E. coli*, *E. faecalis*, and *S. aureus*) in the presence of GO NPs resulted in increased deposition rates and collision efficiency values of the suspended bacteria. However, the multi-parametric dependence of collision efficiency to factors like ionic strength, presence of organic matter, as well as collector and bacterial surface properties, do not permit the prediction of bacterial deposition when GO NPs are present. The presence of GO NPs decreased bacteria mass recovery rates more during their transport than cotransport, suggesting that bacterial co-existence hindered inactivation and deposition processes. However, further investigation is required under various experimental conditions in order to thoroughly understand how attachment and aggregation affect the antibacterial behavior of GO NPs in more complex aquatic environments. Finally, the possibility of using graphene family materials to inhibit the proliferation and inactivation of pathogens may develop new perspectives towards the controlled application of nanotechnology in the fields of health and environmental management.

CRediT authorship contribution statement

Maria P. Georgopoulou: Conceptualization, Data curation, Formal analysis, Writing - original draft. **Vasiliki I. Syngouna:** Methodology, Funding acquisition. **Constantinos V. Chrysikopoulos:** Supervision, Writing - review & editing.

Declaration of Competing Interest

The authors declare that they have no known competing financial interests or personal relationships that could have appeared to influence the work reported in this paper.

Appendix A. Supplementary data

Supplementary data associated with this article can be found, in the online version, at https://doi.org/10.1016/j.colsurfb.2020.110841.

References

[1] C.P. Gerba, J.E. Smith, J. Environ. Qual. 34 (2005) 42–48 (accessed March 1, 2019), http://www.ncbi.nlm.nih.gov/pubmed/15647533.
[2] R. Anders, C.V. Chrysikopoulos, Environ. Sci. Technol. 40 (2006) 3237–3242 (accessed May 21, 2019), http://www.ncbi.nlm.nih.gov/pubmed/16749687.
[3] E. Ramirez, E. Robles, M.E. Gonzalez, M.E. Martinez, Air Soil Water Res. 3 (2010), https://doi.org/10.4137/ASWR.S4823 ASWR.S4823.
[4] P.D. Hynds, M.K. Thomas, K.D.M. Pintar, PLoS One 9 (2014) e93301, , https://doi.org/10.1371/journal.pone.0093301.
[5] G.S. Fout, M.A. Borchardt, B.A. Kieke, M.R. Karim, Hydrogeol. J. 25 (2017) 903–919, https://doi.org/10.1007/s10040-017-1581-5.
[6] B. Nowack, T.D. Bucheli, Environ. Pollut. 150 (2007) 5–22, https://doi.org/10.1016/J.ENVPOL.2007.06.006.
[7] E.J. Petersen, L. Zhang, N.T. Mattison, D.M. O'Carroll, A.J. Whelton, N. Uddin, T. Nguyen, Q. Huang, T.B. Henry, R.D. Holbrook, K.L. Chen, Environ. Sci. Technol. 45 (2011) 9837–9856, https://doi.org/10.1021/es201579y.
[8] M.P. Georgopoulou, C.V. Chrysikopoulos, Ind. Eng. Chem. Res. 57 (2018) 17003–17012, https://doi.org/10.1021/acs.iecr.8b03996.
[9] D.R. Dreyer, S. Park, C.W. Bielawski, R.S. Ruoff, Chem. Soc. Rev. 39 (2010) 228–240, https://doi.org/10.1039/B917103G.
[10] M. Maas, Materials (Basel). 9 (2016) 617, https://doi.org/10.3390/ma9080617.
[11] D.D. Zhou, X.H. Jiang, Y. Lu, W. Fan, M.X. Huo, J.C. Crittenden, Sci. Total Environ. 550 (2016) 717–726, https://doi.org/10.1016/j.scitotenv.2016.01.141.
[12] S.J. Klaine, A.A. Koelmans, N. Horne, S. Carley, R.D. Handy, L. Kapustka, B. Nowack, F. von der Kammer, Environ. Toxicol. Chem. 31 (2012) 3–14, https://doi.org/10.1002/etc.733.
[13] F. von der Kammer, P.L. Ferguson, P.A. Holden, A. Masion, K.R. Rogers, S.J. Klaine, A.A. Koelmans, N. Horne, J.M. Unrine, Environ. Toxicol. Chem. 31 (2012) 32–49, https://doi.org/10.1002/etc.723.
[14] E. Goldberg, M. Scheringer, T.D. Bucheli, K. Hungerbühler, Environ. Sci. Technol. 48 (2014) 12732–12741, https://doi.org/10.1021/es502044k.
[15] Y. Han, C.D. Knightes, D. Bouchard, R. Zepp, B. Avant, H.S. Hsieh, X. Chang, B. Acrey, W. Matthew Henderson, J. Spear, Environ. Sci. Nano 6 (2019) 180–194, https://doi.org/10.1039/C8EN01088A.
[16] V. Palmieri, M. Carmela Lauriola, G. Ciasca, C. Conti, M. De Spirito, M. Papi, Nanotechnology 28 (2017) 152001, , https://doi.org/10.1088/1361-6528/aa6150.
[17] A.B. Seabra, A.J. Paula, R. de Lima, O.L. Alves, N. Durán, Chem. Res. Toxicol. 27 (2014) 159–168, https://doi.org/10.1021/tx400385x.
[18] X. Zou, L. Zhang, Z. Wang, Y. Luo, J. Am. Chem. Soc. 138 (2016) 2064–2077, https://doi.org/10.1021/jacs.5b11411.
[19] A. Al-Jumaili, S. Alancherry, K. Bazaka, M. Jacob, Materials (Basel). 10 (2017) 1066, https://doi.org/10.3390/ma10091066.
[20] Y. Sim, C.V. Chrysikopoulos, Water Resour. Res. 32 (1996) 2607–2611, https://doi.org/10.1029/96WR01496.
[21] Y. Sim, C.V. Chrysikopoulos, Transp. Porous Media 30 (1998) 87–112, https://doi.org/10.1023/A:1006596412177.
[22] N. Tufenkji, Adv. Water Resour. 30 (2007) 1455–1469, https://doi.org/10.1016/J.ADVWATRES.2006.05.014.
[23] S. Torkzaban, S.S. Tazehkand, S.L. Walker, S.A. Bradford, Water Resour. Res. 44 (2008), https://doi.org/10.1029/2007WR006541.
[24] V.I. Syngouna, C.V. Chrysikopoulos, J. Contam, Hydrol. 126 (2011) 301–314, https://doi.org/10.1016/j.jconhyd.2011.09.007.
[25] H. Yang, M. Tong, H. Kim, Environ. Sci. Technol. 47 (2013) 11537–11544, https://doi.org/10.1021/es4022415.
[26] J.D. Lanphere, C.J. Luth, S.L. Walker, Environ. Sci. Technol. 47 (2013) 4255–4261, https://doi.org/10.1021/es400138c.
[27] Y. Sun, B. Gao, S.A. Bradford, L. Wu, H. Chen, X. Shi, J. Wu, Water Res. 68 (2015) 24–33, https://doi.org/10.1016/J.WATRES.2014.09.025.
[28] S. Dong, Y. Sun, B. Gao, X. Shi, H. Xu, J. Wu, J. Wu, Chemosphere. 180 (2017) 506–512, https://doi.org/10.1016/j.chemosphere.2017.04.052.
[29] C.V. Chrysikopoulos, N.P. Sotirelis, N.G. Kallithrakas-Kontos, Transp. Porous Media 119 (2017) 181–204, https://doi.org/10.1007/s11242-017-0879-z.
[30] C. Zhang, A. Yan, G. Wang, C. Jin, Y. Chen, C. Shen, Vadose Zone J. 17 (2018), https://doi.org/10.2136/vzj2018.01.0019.
[31] M. Wang, B. Gao, D. Tang, C. Yu, Environ. Pollut. 235 (2018) 350–357, https://doi.org/10.1016/j.envpol.2017.12.063.
[32] V.I. Syngouna, C.V. Chrysikopoulos, Colloids Surfaces A Physicochem. Eng. Asp. 416 (2013) 56–65, https://doi.org/10.1016/J.COLSURFA.2012.10.018.
[33] V.E. Katzourakis, C.V. Chrysikopoulos, Adv. Water Resour. 68 (2014) 62–73, https://doi.org/10.1016/J.ADVWATRES.2014.03.001.
[34] V.I. Syngouna, C.V. Chrysikopoulos, J. Colloid Interface Sci. 440 (2015) 140–150, https://doi.org/10.1016/J.JCIS.2014.10.066.
[35] M.I. Bellou, V.I. Syngouna, M.A. Tselepi, P.A. Kokkinos, S.C. Paparrodopoulos, A. Vantarakis, C.V. Chrysikopoulos, Sci. Total Environ. 517 (2015) 86–95, https://doi.org/10.1016/j.scitotenv.2015.02.036.
[36] V.I. Syngouna, C.V. Chrysikopoulos, J. Colloid Interface Sci. 497 (2017) 117–125, https://doi.org/10.1016/j.jcis.2017.02.059.
[37] S.M. Notley, R.J. Crawford, E.P. Ivanova, Chapter 5 Bacterial Interaction With Graphene Particles and Surfaces, (2013) (accessed June 14, 2019), https://www.semanticscholar.org/paper/Chapter-5-Bacterial-Interaction-with-Graphene-and-Notley-Crawford/b542045123749354beeb0f955197844756fc3633.
[38] R.F. Al-Thani, N.K. Patan, M.A. Al-Maadeed, R.F. Al-Thani, N.K. Patan, M.A. Al-Maadeed, Online J. Biol. Sci. 14 (2014) 230–239, https://doi.org/10.3844/ojbsci.2014.230.239.
[39] V. Palmieri, F. Bugli, M.C. Lauriola, M. Cacaci, R. Torelli, G. Ciasca, C. Conti, M. Sanguinetti, M. Papi, M. De Spirito, ACS Biomater. Sci. Eng. 3 (2017) 619–627, https://doi.org/10.1021/acsbiomaterials.6b00812.
[40] M.U. Farid, J. Guo, A.K. An, J. Memb. Sci. 564 (2018) 22–34, https://doi.org/10.1016/J.MEMSCI.2018.06.061.
[41] J. Jira, B. Rezek, V. Kriha, A. Artemenko, I. Matolínová, V. Skakalova, P. Stenclova, A. Kromka, Nanomaterials 8 (2018) 140, https://doi.org/10.3390/nano8030140.
[42] Z. Ge, D. Wu, L. He, X. Liu, M. Tong, Sci. China Ser. A-mathematics Phys. Astron. Technol. Sci. 62 (2019) 276–286, https://doi.org/10.1007/s11431-018-9298-x.
[43] N.B. DeFelice, J.E. Johnston, J.M. Gibson, Environ. Sci. Technol. 49 (2015) 10019–10027, https://doi.org/10.1021/acs.est.5b01898.
[44] I. Chowdhury, M.C. Duch, N.D. Mansukhani, M.C. Hersam, D. Bouchard, Environ. Sci. Technol. 47 (2013) 6288–6296, https://doi.org/10.1021/es400483k.
[45] A.L. Barry, R.E. Badal, R.W. Hawkinson, J. Clin. Microbiol. 18 (1983) 645–651 (accessed April 15, 2019), http://www.ncbi.nlm.nih.gov/pubmed/6605360.
[46] S. Sutton, Microbiology Topics, Measurement of Microbial Cells by Optical Density, (2011) (accessed April 15, 2019), www.microbiol.org.
[47] I. George, P. Crop, P. Servais, Water Res. 36 (2002) 2607–2617, https://doi.org/10.1016/S0043-1354(01)00475-4.
[48] N.P. Sotirelis, C.V. Chrysikopoulos, Environ. Sci. Technol. 49 (2015) 13413–13421, https://doi.org/10.1021/acs.est.5b03496.
[49] N.P. Sotirelis, C.V. Chrysikopoulos, Sci. Total Environ. 579 (2017) 736–744, https://doi.org/10.1016/j.scitotenv.2016.11.034.
[50] K. He, G. Chen, G. Zeng, M. Peng, Z. Huang, J. Shi, T. Huang, Nanoscale 9 (2017) 5370–5388, https://doi.org/10.1039/c6nr09931a.
[51] Y. Liang, S.A. Bradford, J. Šimůnek, E. Klumpp, Sci. Total Environ. 656 (2019) 70–79, https://doi.org/10.1016/j.scitotenv.2018.11.258.
[52] Database) Typical Soil Parameters Properties (2014) | Geotechnical Engineering | Mechanical Engineering, (n.d.). https://www.scribd.com/doc/271832045/Database-Typical-Soil-Parameters-Properties-2014 (accessed March 6, 2019).
[53] C.V. Chrysikopoulos, V.I. Syngouna, Environ. Sci. Technol. 48 (2014) 6805–6813, https://doi.org/10.1021/es501295n.
[54] V.E. Katzourakis, C.V. Chrysikopoulos, Groundwater 55 (2017) 156–159, https://doi.org/10.1111/gwat.12501.
[55] Y. Sim, C.V. Chrysikopoulos, Water Resour. Res. 31 (1995) 1429–1437, https://doi.org/10.1029/95WR00199.
[56] P.N. Mitropoulou, V.I. Syngouna, C.V. Chrysikopoulos, Chem. Eng. J. 232 (2013) 237–248, https://doi.org/10.1016/J.CEJ.2013.07.093.
[57] R. Rajagopalan, C. Tien, AIChE J. 22 (1976) 523–533, https://doi.org/10.1002/aic.690220316.
[58] N. Tufenkji, M. Elimelech, Environ. Sci. Technol. 38 (2004) 529–536 (accessed April 12, 2019), http://www.ncbi.nlm.nih.gov/pubmed/14750730.
[59] C.V. Chrysikopoulos, V.I. Syngouna, Colloids Surf. B Biointerfaces 92 (2012) 74–83, https://doi.org/10.1016/j.colsurfb.2011.11.028.
[60] T. Wu, C. Zhai, J. Zhang, D. Zhu, K. Zhao, Y. Chen, T. Wu, C. Zhai, J. Zhang, D. Zhu, K. Zhao, Y. Chen, Water 11 (2019) 819, https://doi.org/10.3390/w11040819.
[61] J.C. Baygents, J.R. Glynn, O. Albinger, B.K. Biesemeyer, K.L. Ogden, R.G. Arnold, Environ. Sci. Technol. 32 (1998) 1596–1603, https://doi.org/10.1021/es9707116.
[62] M. Wang, B. Gao, D. Tang, H. Sun, X. Yin, C. Yu, J. Hazard. Mater. 331 (2017) 28–35, https://doi.org/10.1016/j.jhazmat.2017.02.014.
[63] L. Feriancikova, S. Xu, J. Hazard. Mater. 235–236 (2012) 194–200, https://doi.org/10.1016/j.jhazmat.2012.07.041.
[64] Y. Wang, B. Gao, V.L. Morales, Y. Tian, L. Wu, J. Gao, W. Bai, L. Yang, J. Nanopart. Res. 14 (2012) 1095, https://doi.org/10.1007/s11051-012-1095-y.
[65] J. Díaz, M. Rendueles, M. Díaz, Environ. Sci. Pollut. Res. 17 (2010) 400–409, https://doi.org/10.1007/s11356-009-0160-2.
[66] A. Santos, P.H.L. Barros, Environ. Sci. Technol. 44 (2010) 2515–2521, https://doi.org/10.1021/es9034792.
[67] M. Wang, R.M. Ford, Environ. Sci. Technol. 43 (2009) 5921–5927, https://doi.org/10.1021/es901001t.
[68] X. Wang, L.M. Lanning, R.M. Ford, Environ. Sci. Technol. 50 (2016) 165–172, https://doi.org/10.1021/acs.est.5b03872.
[69] L. Yang, X. Chen, X. Zeng, M. Radosevich, S. Ripp, J. Zhuang, G.S. Sayler, Front. Microbiol. 10 (2019), https://doi.org/10.3389/fmicb.2019.02691.
[70] A.J. De Kerchove, M. Elimelech, Appl. Environ. Microbiol. 73 (2007) 5227–5234, https://doi.org/10.1128/AEM.00678-07.
[71] S. Peng, D. Wu, Z. Ge, M. Tong, H. Kim, Environ. Pollut. 225 (2017) 141–149, https://doi.org/10.1016/J.ENVPOL.2017.03.064.
[72] G. Chen, S.L. Walker, Environ. Sci. Technol. 46 (2012) 8782–8790, https://doi.org/10.1021/es301378q.
[73] H. Zhong, G. Liu, Y. Jiang, J. Yang, Y. Liu, X. Yang, Z. Liu, G. Zeng, Biotechnol. Adv. 35 (2017) 490–504, https://doi.org/10.1016/j.biotechadv.2017.03.009.

[74] A. Bozorg, I.D. Gates, A. Sen, J. Microbiol, Methods. 109 (2015) 84–92, https://doi.org/10.1016/j.mimet.2014.11.015.
[75] D. Janjaroen, F. Ling, G. Monroy, N. Derlon, E. Mogenroth, S.A. Boppart, W.-T. Liu, T.H. Nguyen, W.-T. Liu, T.H. Nguyen, Water Res. 47 (2013) 2531–2542, https://doi.org/10.1016/j.watres.2013.02.032.
[76] B.E. Rittmann, J. Am. Water Works Assoc. 82 (1990) 62–66, https://doi.org/10.1002/j.1551-8833.1990.tb07068.x.
[77] R.L. Whitman, V.J. Harwood, T.A. Edge, M.B. Nevers, M. Byappanahalli, K. Vijayavel, J. Brandão, M.J. Sadowsky, E.W. Alm, A. Crowe, D. Ferguson, Z. Ge, E. Halliday, J. Kinzelman, G. Kleinheinz, K. Przybyla-Kelly, C. Staley, Z. Staley, H.M. Solo-Gabriele, Rev. Environ. Sci. Biotechnol. 13 (2014) 329–368, https://doi.org/10.1007/s11157-014-9340-8.
[78] O. Akhavan, E. Ghaderi, ACS Nano 4 (2010) 5731–5736, https://doi.org/10.1021/nn101390x.
[79] L. Xu, R. Ma, C. Sun, D. Sun, Polish J. Environ. Stud. 27 (2018) 2811–2820, https://doi.org/10.15244/pjoes/81267.
[80] M. Tong, G. Long, X. Jiang, H.N. Kim, Environ. Sci. Technol. 44 (2010) 2393–2399, https://doi.org/10.1021/es9027937.
[81] K. Shellenberger, B.E. Logan, Environ. Sci. Technol. 36 (2002) 184–189 (accessed June 13, 2019), http://www.ncbi.nlm.nih.gov/pubmed/11827052.
[82] W. Richard Bowen, T.A. Doneva, J. Colloid Interface Sci. 229 (2000) 544–549, https://doi.org/10.1006/JCIS.2000.6997.
[83] W.R. Bowen, T.A. Doneva, J.A.G. Stoton, Colloids Surfaces A Physicochem. Eng. Asp. 201 (2002) 73–83, https://doi.org/10.1016/S0927-7757(01)00790-7.
[84] E.M.V. Hoek, S. Bhattacharjee, M. Elimelech, Langmuir 19 (2003) 4836–4847, https://doi.org/10.1021/la027083c.
[85] S. Chakraborty, S. Mukherji, S. Mukherji, Colloids Surf. B Biointerfaces 78 (2010) 101–108, https://doi.org/10.1016/j.colsurfb.2010.02.019.
[86] J. Macko, A. Oriňak, R. Oriňaková, C. Muhmann, O. Petruš, D. Harvanová, J. Vargová, R. Jendželovský, J. Radoňák, P. Fedoročko, H.F. Arlinghaus, Appl. Surf. Sci. 355 (2015) 553–561, https://doi.org/10.1016/J.APSUSC.2015.07.104.
[87] L. Wang, T. Yue, Y. Yuan, Z. Wang, M. Ye, R. Cai, Food Control 50 (2015) 104–110, https://doi.org/10.1016/J.FOODCONT.2014.08.041.
[88] H. Zhong, Y. Jiang, G. Zeng, Z. Liu, L. Liu, Y. Liu, X. Yang, M. Lai, Y. He, J. Hazard. Mater. 285 (2015) 383–388, https://doi.org/10.1016/j.jhazmat.2014.11.050.
[89] R.-H. Yoon, D.H. Flinn, Y.I. Rabinovich, J. Colloid Interface Sci. 185 (1997) 363–370, https://doi.org/10.1006/JCIS.1996.4583.